

# Synchrony in Broadband Fluctuation and the 2008 Financial Crisis

Der Chyan Lin\*

Department of Mechanical and Industrial Engineering, Ryerson University, Toronto, Ontario, Canada

## Abstract

We propose phase-like characteristics in scale-free broadband processes and consider fluctuation synchrony based on the temporal signature of significant amplitude fluctuation. Using wavelet transform, successful captures of similar fluctuation pattern between such broadband processes are demonstrated. The application to the financial data leading to the 2008 financial crisis reveals the transition towards a qualitatively different dynamical regime with many equity price in fluctuation synchrony. Further analysis suggests an underlying scale free “price fluctuation network” with large clustering coefficient.

**Citation:** Lin DC (2013) Synchrony in Broadband Fluctuation and the 2008 Financial Crisis. PLoS ONE 8(10): e77254. doi:10.1371/journal.pone.0077254

**Editor:** Francesco Pappalardo, University of Catania, Italy

**Received:** April 25, 2013; **Accepted:** September 1, 2013; **Published:** October 28, 2013

**Copyright:** © 2013 Der Chyan Lin. This is an open-access article distributed under the terms of the Creative Commons Attribution License, which permits unrestricted use, distribution, and reproduction in any medium, provided the original author and source are credited.

**Funding:** Natural Science and Engineering Research Council of Canada. The funders had no role in study design, data collection and analysis, decision to publish, or preparation of the manuscript.

**Competing Interests:** The author has declared that no competing interests exist.

\* E-mail: derlin@ryerson.ca

## Introduction

Synchrony among coupled oscillators has fascinated scientists and engineers for decades. There is an extensive literature on the subject, from Huygen’s clock [1], amplitude, phase synchronization of low-dimensional systems [2], Kuramoto phase oscillators [3], to diverse manifestations in natural phenomena, such as social opinion formation [4–7], population of species [8,9], collective motion of Starling flock [10], traffic [11], neuronal dynamics [12,13], just to name a few. Synchrony between broadband processes is more subtle for it can emerge, disappear and reappear sporadically in time, and is difficult to identify for it is less exact; i.e., only similar fluctuation pattern may exist. Of interest here is the synchrony between broadband processes showing scale free characteristics. The fluctuation of the process has therefore a power law characterization, such as the power law power spectrum. In this work, we propose the state of *fluctuation in synchrony* [14] (FIS) between broadband processes and present a wavelet method to derive phase-like quantity to study FIS.

One area where FIS likely occurs is the market dynamics. Equity price is known to exhibit broadband fluctuation and fractal property [15,16]. Besides the market fundamental, a broad base price increase or drop suggests the possibility of FIS. The goal of this work is to study FIS of the dramatic equity price fluctuation in the 2008 financial crisis. We find that the FIS among price series exhibits a bifurcation pattern at the crisis. Using a network analogy, we further show that the market dynamics underlying FIS has a scale free configuration and a large clustering coefficient.

## Methods

Our approach relies on the so-called wavelet transform modulus maxima line (WTMML). For square-integrable function or bounded signal in practice, wavelet transform can effectively describe the local fluctuation according to the scale of resolution [17,18]. The use of wavelet transform as a signal processing tool to describe scale free property has a long history [17–19]. WTMM

was initially motivated for improved understandings of the hydrodynamic turbulence, but was soon realized to have much wider application for natural processes in diverse fields. The main idea is based on the concept of singularity in mathematics where scale free property can be obtained from the wavelet coefficients along the WTMML. Our objective is slightly different in that we are mainly interested in the location of the WTMML. On the wavelet time-scale plane  $t \times s$ , WTMML is a connected curve defined by the modulus maxima of the continuous wavelet transform coefficient  $|x * \psi_s(t)|$ , where  $x(t)$  is the time series of interest, a “\*” denotes the convolution, and  $\psi_s(t) = \psi(t/s)/s$  is the dilated analyzing wavelet  $\psi(t)$  satisfying  $\int \psi(t)dt = 0$  [17]. We

shall denote these WTMML locations at the smallest scale by  $\tau_i, i \in \mathbb{Z}$ , and refer to them as the *WTMML roots*. Huang and Mallet proved the seminal result on the convergence of  $\tau_i$ ’s towards (singularity) locations where the derivative of the function is undefined [17]; see also Ref [19]. Intuitively, these are where the time series exhibits abrupt changes or jumps in the amplitude fluctuation. By identifying such feature as the phase setting event,  $\tau_i$  maybe used to derive the phase difference of the fluctuation of broadband processes. Specifically, let  $R_x = \{\tau_i^{(x)}\}$ ,  $R_y = \{\tau_j^{(y)}\}$  be the WTMML roots of time series  $x(t), y(t)$ , respectively. The first step in the FIS analysis is to search for nearest WTMML roots, say  $\tau_m^{(x)}, \tau_n^{(y)}$ , satisfying  $\delta = \min_{i,j} (|\tau_i^{(x)} - \tau_j^{(y)}|) = |\tau_m^{(x)} - \tau_n^{(y)}|$  (FIG. 1b below). Once such nearest WTMML roots are found, they are deleted from  $R_{x,y}$  and the search continues until all WTMML roots are processed. The  $\delta$  so obtained captures the difference in “timing” of the large amplitude jumps of  $x, y$ , and is used as the measure for the phase difference of the fluctuation.

When all WTMML roots of  $x, y$  are separated by a fixed distance,  $\delta$  equals a constant and has a Dirac delta probability density function (PDF)  $p(\delta)$ . In this case, the FIS is said to be *complete*. As the FIS level drops, the WTMML roots are more scattered and the shape of  $p(\delta)$  widens. To measure FIS, we use an

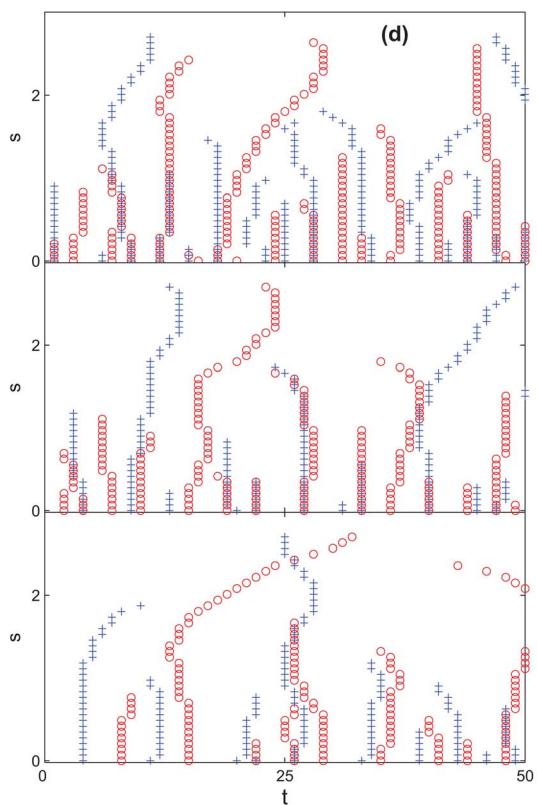
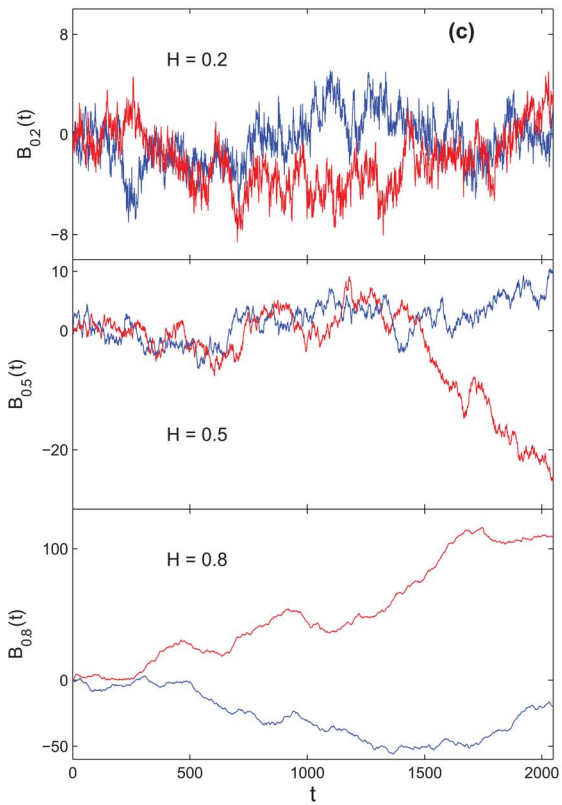
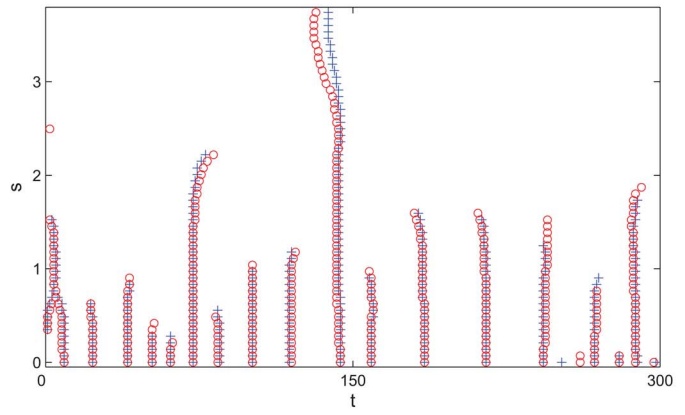
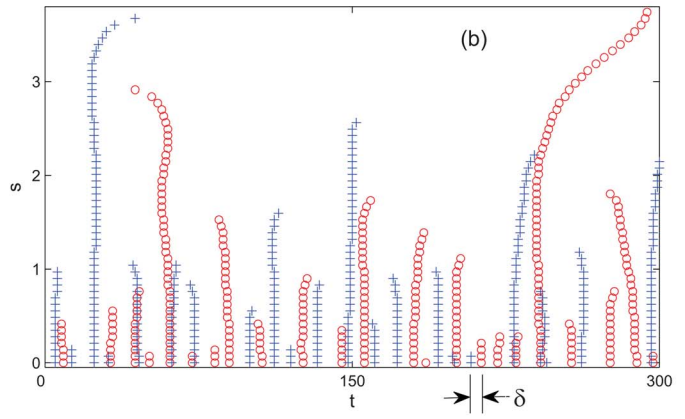
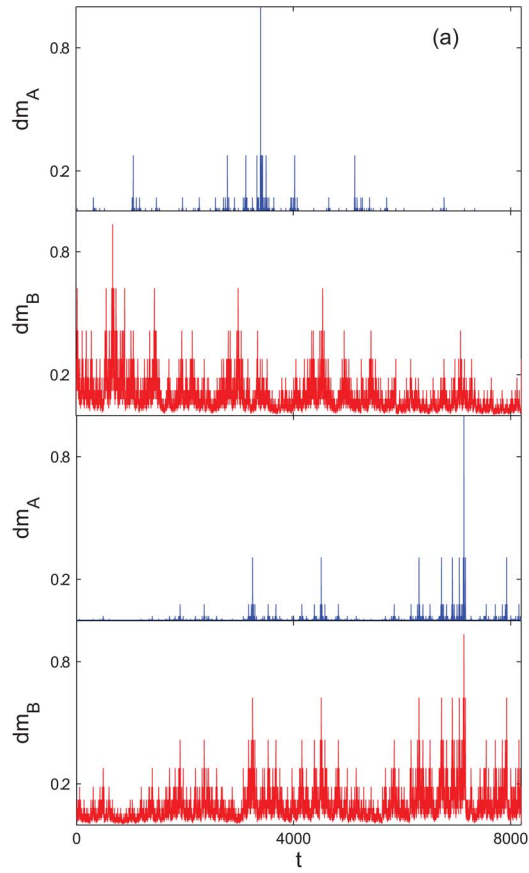


**Figure 1. FIS in artificial examples.** (a) Cascade  $dm_{A,B}$  for  $z=0.2$  (top two panels) and  $z=1.0$  (bottom two panels). Notice the more (synchronized) similar fluctuation pattern as  $z$  increases to 1. (b) WTMM's of  $m_A$  ("+"),  $m_B$  ("o") constructed from (a) with  $z=0.2$  (top) and  $z=1.0$  (bottom). (c) Two samples (one in blue and one in red) of  $B_H$  for  $H=0.2,0.5,0.8$  (top to bottom). (d) WTMM's of  $B_H$ 's shown in (c): ("+" for the blue sample and "o" for the red sample).  
doi:10.1371/journal.pone.0077254.g001

**Table 1. Average  $\rho(z)$  with 1 standard deviation (SD) based on the ensemble of 30 pairs of  $m_{A,B}$ .**

| g                    | 0.0               | 0.2               | 0.4               | 0.6               | 0.8               | 1.0               |
|----------------------|-------------------|-------------------|-------------------|-------------------|-------------------|-------------------|
| $\rho \pm \text{SD}$ | 0.661 $\pm$ 0.003 | 0.674 $\pm$ 0.004 | 0.695 $\pm$ 0.005 | 0.732 $\pm$ 0.005 | 0.797 $\pm$ 0.006 | 0.952 $\pm$ 0.032 |

doi:10.1371/journal.pone.0077254.t001

entropy based synchronization index (SI) [20]:  $\rho = (S_{\max} - S) / S_{\max}$  where  $S = -\sum p \log(p)$  is the Shannon entropy and  $S_{\max} = \log(N_0)$  is the largest entropy from a uniformly distributed  $\delta$ . Thus,  $\rho = 1$  for a Dirac delta  $p(\delta)$  in complete FIS and  $\rho \rightarrow 0$  for completely independent fluctuations.

In the numerical analysis, the  $k$ th order gaussian derivative wavelet  $g_k$  is considered. Since  $g_k$  has  $k$  vanishing moments, it is able to capture irregularities in the  $(k-1)$ th derivative of a function. However, for defining the phase event, wavelet with higher order vanishing moment may be too sensitive, resulting in WTMM roots at every "regular" rise-and-fall of the time series. To capture more "violent" fluctuation pattern that is typically found in the financial data, using analyzing wavelets with the lowest number of vanishing moment is more desirable. In this study,  $g_1 = (d/dt) \exp(-t^2/2)$  is used.

### Results

We will first apply the above ideas to demonstrate FIS using artificial time series. Consider multifractal measures  $m_A, m_B$ , where  $dm_A = \pi_A(t; w_0^{(A)}, w_1^{(A)})$ ,  $dm_B = \pi_B(t; w_0^{(B)}, w_1^{(B)})$ , are dyadic cascades with deterministic weights  $w_{0,1}^{(A)}, w_{0,1}^{(B)}$  satisfying  $\sum_i w_i^{(A)} = \sum_i w_i^{(B)} = 1$ . Let the weights be assigned randomly, say, by flipping a coin, to dyadic intervals. One can write  $\pi_\alpha(t) = \prod_{J_\alpha(t)} w_k^{(\alpha)}$ ,  $\alpha = A, B$ , where  $J_\alpha(t)$  is a random sequence of 0,1. FIS is realized by ensuring  $J_A(t) = J_B(t)$  in some time interval. This may be achieved by imposing  $J_A(t) = J_B(t)$  whenever a uniformly distributed  $\zeta$  in  $[0,1]$  is less than a constant  $z$ . Thus,  $m_{A,B}$  are independent when  $z=0$  and in complete FIS when  $z \geq 1$ . The function  $\rho(z)$  is therefore increasing in  $z$ . To demonstrate, 30 pairs of  $m_{A,B}$  of 8,192 points each were generated with  $w_{0,1}^{(A)} = (0.2, 0.8)$ ,  $w_{0,1}^{(B)} = (0.4, 0.6)$  for  $z=0$  to 1 in 0.2 increment. Indeed, it is observed that the WTMM roots are more scattered at  $z=0$  and have almost identical locations at  $z=1$  (FIGs. 1a, 1b). They lead to the increasing  $\rho(z)$  as predicted (TABLE 1).

While  $\delta$  is motivated to measure the phase difference, it also characterizes the intrinsic property of the broadband fluctuation. Consider the fractional Brownian motion (fBm)  $B_H(t)$  [21]. With

probability 1,  $B_H$  is continuous and nowhere differentiable; i.e., it is singular almost everywhere (Lipschitz exponent less than 1). Its covariance function given by  $(|t|^{2H} + |s|^{2H} - |t-s|^{2H})/2$  implies a negatively (positively) correlated increment  $\Delta B_H(d) = B_H(t+d) - B_H(t)$  for  $H < 0.5$  ( $H > 0.5$ ). For a fixed  $H$ , we conducted the FIS analysis based on different realizations of  $B_H$  and found a decreasing  $\rho(H)$ ; see FIGs. 1c, 1d and TABLE 2). This result follows intuitively from  $\Delta B_H$ . Since the singularity in  $B_H$  arises mostly from a positive increment followed by a negative one, or vice versa, there are relatively more WTMM roots for  $H < 0.5$  (with negatively correlated increment). This implies a smaller  $\delta$  range, or narrower  $p(\delta)$ , and thus a larger  $\rho$  value.

We now apply these ideas to analyze the fluctuation in the equity price series. The daily closing price,  $x_{C,1}, \dots, x_{C,N}$ , for  $N=250$  publicly traded stocks in NASDAQ from Jan 2001 to Nov 2011 are used (File S1). This selection is aimed at a reasonable mix of the market, so that any potential FIS represents a general market property, rather than the characteristics of a particular business sector. FIG. 2a shows the broadband character of the price series where the power-law power spectrum can be clearly seen. FIGs. 2b~2d shows the typical case that suggests FIS in the market dynamics. They are the closing price of two technology companies  $x_{C,1}$  (Agilent Tech Inc) and  $x_{C,4}$  (Analog Devices Inc), where similar fluctuation pattern is visually apparent. But similar fluctuation patterns exist more generally in companies from different sectors, for example, those between  $x_{C,4}$  and  $x_{C,60}$  of an energy company (CenterPoint Energy Inc).

To analyze the potential FIS in the price series, we take into account the market nonstationarity by processing the data in window segments of  $L$  calendar year, advancing every  $V$  calendar month ( $V < L$ ). In general, using smaller  $L, V$  suffers from poorer statistics and results in larger fluctuation of the SI  $\rho$ . But using larger  $L, V$  can average out the subtle fluctuation in the market dynamics. Our goal is to find persistent FIS indicators over a reasonable range of  $V, L$ . These indicators are now described.

Given  $N$  price series, there are  $N(N-1)/2$  sets of  $p(\delta)$ 's are obtained in each of the window segment (31,125 sets for  $N=250$ ). They were then used to calculate the pair-wise SI  $\rho_{i,j}, i, j = 1, \dots, N$ . The FIS indicators used in this study are defined from the  $\rho_{i,j}$ . First, the sample mean and standard variance  $\bar{\rho}_i = \sum_{j \neq i} \rho_{i,j} / (N-1)$ ,  $\bar{\sigma}_i^2 = \sum_{j \neq i} (\rho_{i,j} - \bar{\rho}_i)^2 / (N-2)$ , respectively, are calculated for the  $i$ th price series. Then, averages are made to define the FIS indicators  $\mu_\rho = \sum_i \bar{\rho}_i / N$  and  $\sigma_\rho = \sqrt{\sum_i \bar{\sigma}_i^2 / N}$ .

A large  $\mu_\rho$  implies a higher FIS level market. But it does not mean the formation of a global cluster of companies that exhibit similar price fluctuation. If  $\sigma_\rho$  is also large, smaller clusters are

**Table 2. Average  $\rho(H)$  with 1 standard deviation (SD) based on 30 samples of  $B_H$  at  $H=0.2,0.5,0.8$ .**

| H                    | 0.2               | 0.5               | 0.8               |
|----------------------|-------------------|-------------------|-------------------|
| $\rho \pm \text{SD}$ | 0.581 $\pm$ 0.009 | 0.506 $\pm$ 0.012 | 0.423 $\pm$ 0.011 |

doi:10.1371/journal.pone.0077254.t002

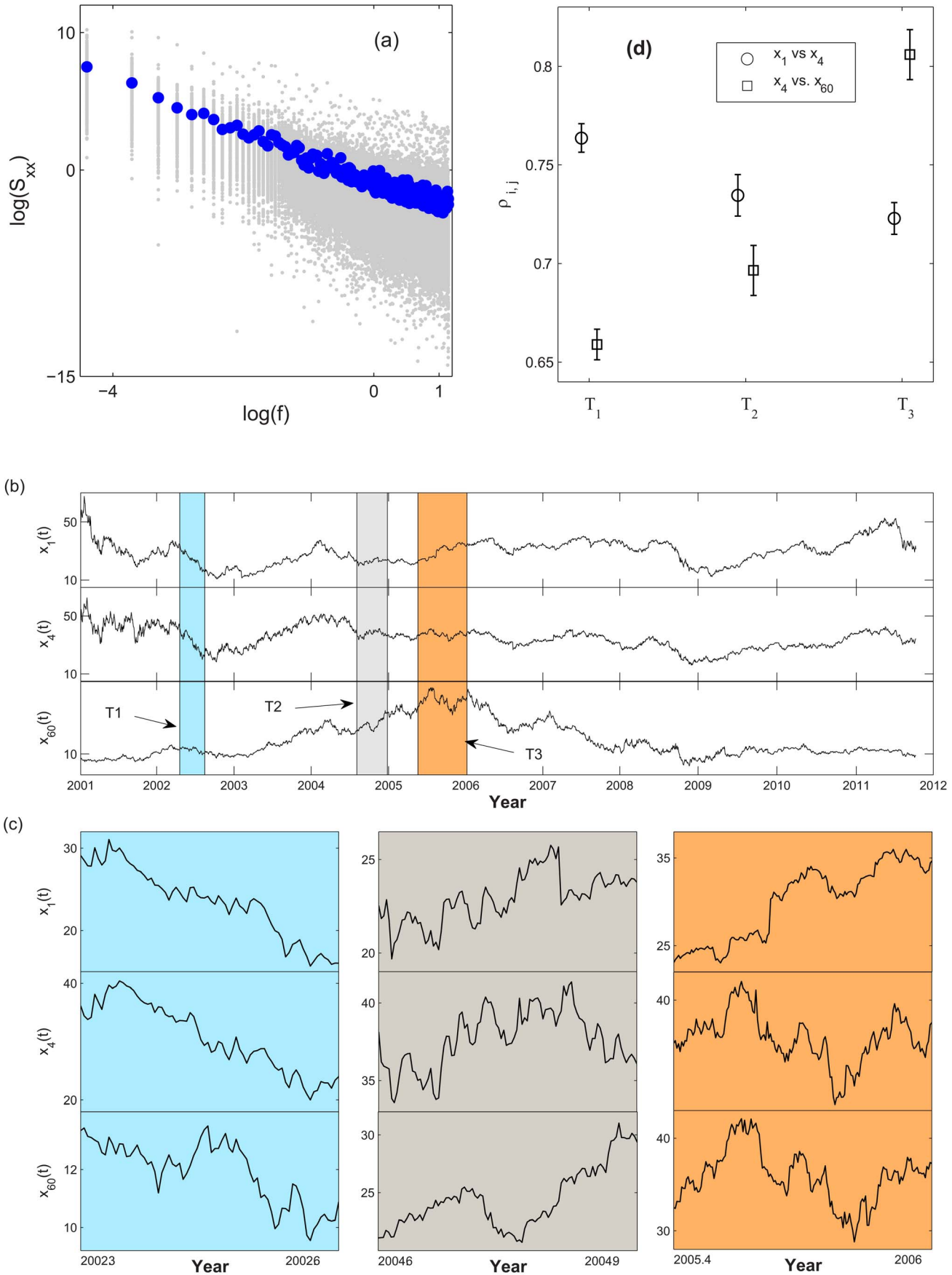


**Figure 2. FIS in equity price series.** (a) Power law power spectra of all price series (●, grey) and their average (●, blue), (b) Examples of price series  $x_{C,1}, x_{C,4}, x_{C,60}$  (top to bottom). Typical FIS is demonstrated in three selected time intervals:  $T_1 = 2002.3 \sim 2002.6$  Yr (left, blue background),  $T_2 = 2004.6 \sim 2004.9$  Yr (middle, grey background),  $T_3 = 2005.4 \sim 2006$  Yr (right, orange background). (c) Zoom-in of the price fluctuation of the price series in  $T_1, T_2, T_3$  (left to right). (d) Pair-wise  $\rho_{1,4}$  ("o"),  $\rho_{4,60}$  ("□") in  $T_1, T_2, T_3$  (left to right). Calculations are based on  $L=2, V=1$ . Error bars correspond to one standard deviation of the  $\rho_{ij}$  values in  $T_1, T_2, T_3$ . doi:10.1371/journal.pone.0077254.g002

likely formed. This is because, while  $\rho_{ij}$  for  $x_{C,i}, x_{C,j}$  in the same cluster increases, the  $\rho_{ij}$  with the price series  $x_{C,j'}$  from a different cluster decreases, which in turn creates a greater disparity of the pair-wise SI and, thus, a larger  $\sigma_\rho$ .

FIGS. 3a, 3b present the FIS indicators that characterize the market synchrony. They show the  $\mu_\rho, \sigma_\rho$  obtained by using window parameters  $L=2, V=1$ . Most notably here is the rise of  $\mu_\rho, \sigma_\rho$  at apparently a transition year  $T_* \sim 2007.5$  Yr. Let  $T_*$  define a

pre- and post-2008 regimes in reference to the 2008 financial crisis. A closer examination reveals a bifurcation pattern, where  $\sigma_\rho$  considered as a function of  $\mu_\rho$  first clusters around a steady range in the pre-2008 regime and then bifurcates into at least two branches in the post-2008 regime (FIG 3c). The rising  $\mu_\rho$  and  $\sigma_\rho$  after  $T_*$  suggest the formation of smaller clusters of  $x_{C,i}$ 's showing similar price fluctuation. The top branch in the post-2008 regime started at around the third quarter of 2009. It is when  $\mu_\rho$  begins to

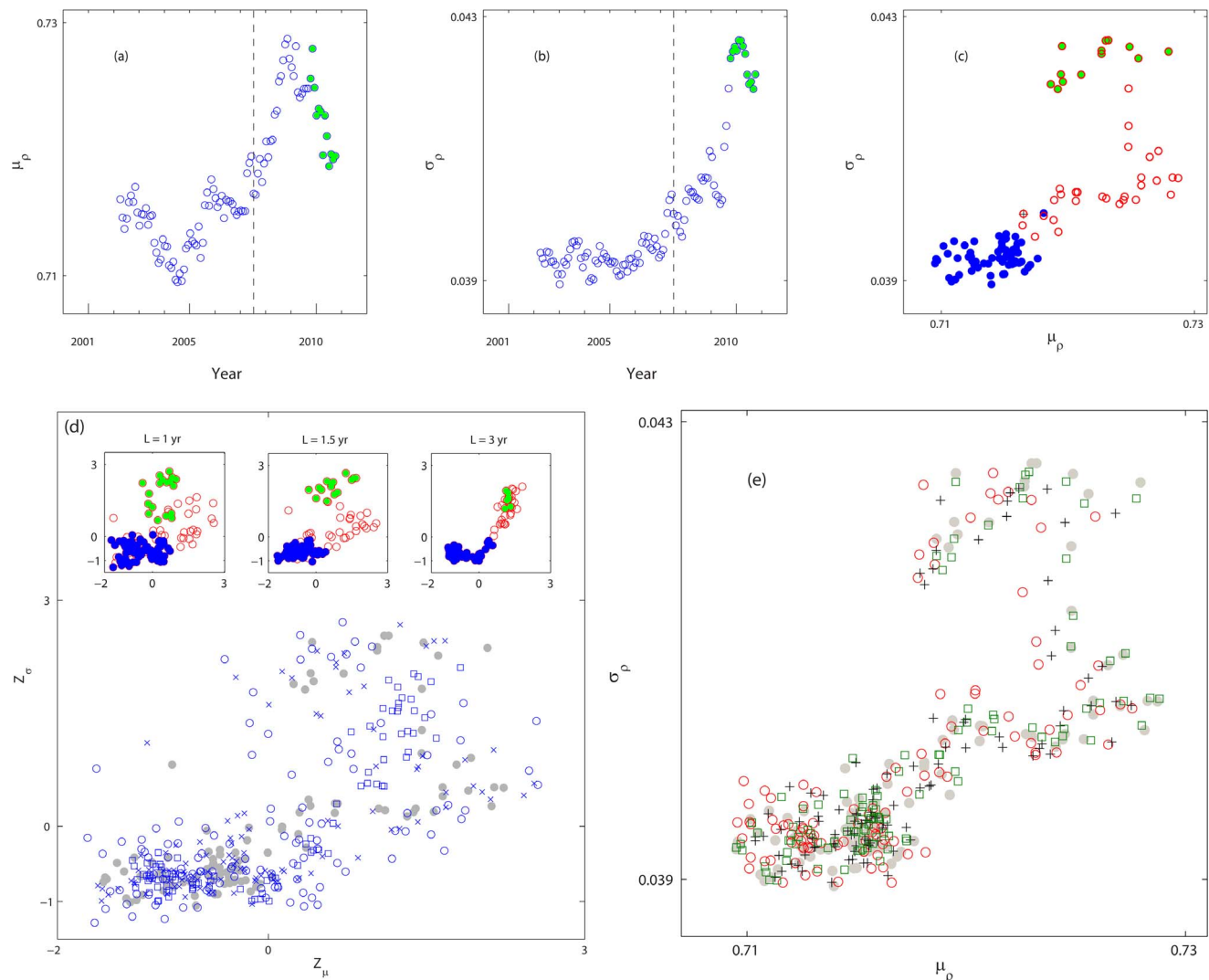


**Figure 3. FIS indicators of the price series obtained by using window parameters  $L=2, V=1$  from 2001 to 2011.** (a)  $\mu_\rho$ , (b)  $\sigma_\rho$ , (c)  $\mu_\rho$  vs.  $\sigma_\rho$ . The transition year  $T_* = 2007.5$  is marked by the long-dashed line in (a), (b) and by a cross + in (c). In (c), blue filled circles, and red open circles correspond to the pre- and post-2008 regimes. In (a)~(c), green filled circles correspond to the top branch of the bifurcation pattern. (d) FIS indicators obtained by using different window lengths  $L=1$  ("o"),  $1.5$  ("x"),  $2$  ("●", grey) and  $3$  ("□") and  $V=1$ . To facilitate the comparison,  $\sigma_\rho$  vs.  $\mu_\rho$  are normalized according to  $Z_\mu = (\mu_\rho - \text{MEAN}(\mu_\rho)) / \sqrt{\text{VAR}(\mu_\rho)}$  and  $Z_\sigma = (\sigma_\rho - \text{MEAN}(\sigma_\rho)) / \sqrt{\text{VAR}(\sigma_\rho)}$  where MEAN, VAR denote the sample mean and variance, respectively. The insets show the transition separating the pre- and post-2008 regimes using the same color scheme as (c). (e)  $\mu_\rho$  vs.  $\sigma_\rho$  for the first 100 stocks ("o", red), 150 ("+", black), 200 ("□", green). The result of 250 stocks shown in (c) is added for comparison ("●", grey). doi:10.1371/journal.pone.0077254.g003

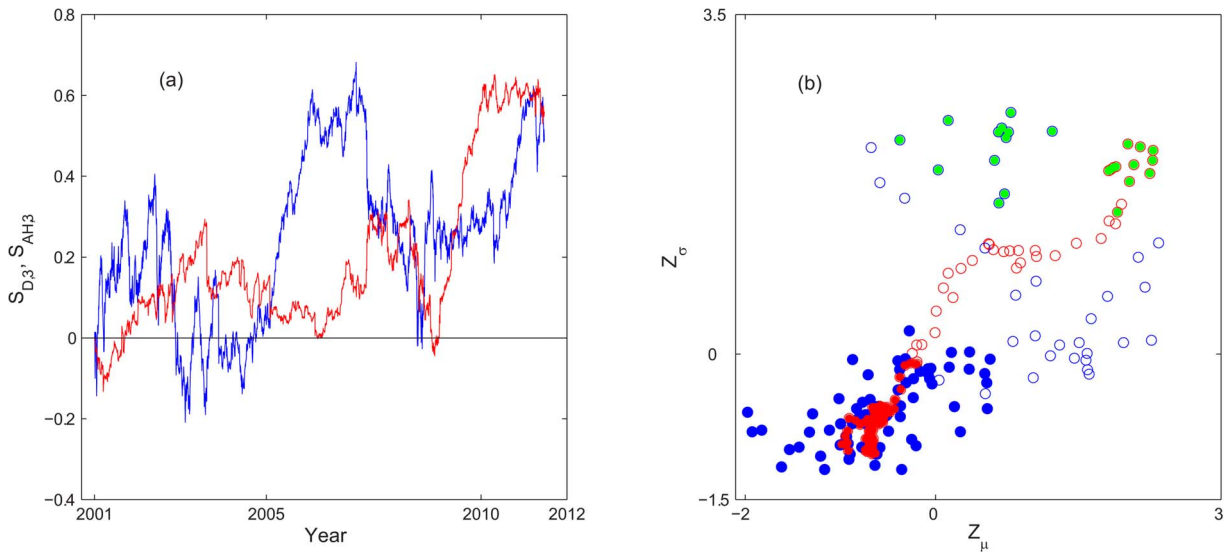


**Figure 4. FIS indicators of the cumulative returns.** (a) Examples of cumulative daily and after-hour returns for a pharmaceutical services company (AmerisourceBergen Corp),  $S_{D,3}(t)$  (blue) and  $S_{AH,3}(t)$  (red). (b) FIS indicators of  $\{S_{D,i}, i=1, \dots, N\}$  (blue) and  $\{S_{AH,i}, i=1, \dots, N\}$  (red). The indicators are normalized:  $Z_\mu = (\mu_p - MEAN(\mu_p)) / \sqrt{VAR(\mu_p)}$  and  $Z_\sigma = (\sigma_p - MEAN(\sigma_p)) / \sqrt{VAR(\sigma_p)}$ . The pre-, post-2008 regimes are shown using the similar specification as FIG. 3c: pre-2008 regime in filled circles, post-2008 regime in open circles, and solid green circles from the period of the top branch in FIG. 3c.  
doi:10.1371/journal.pone.0077254.g004

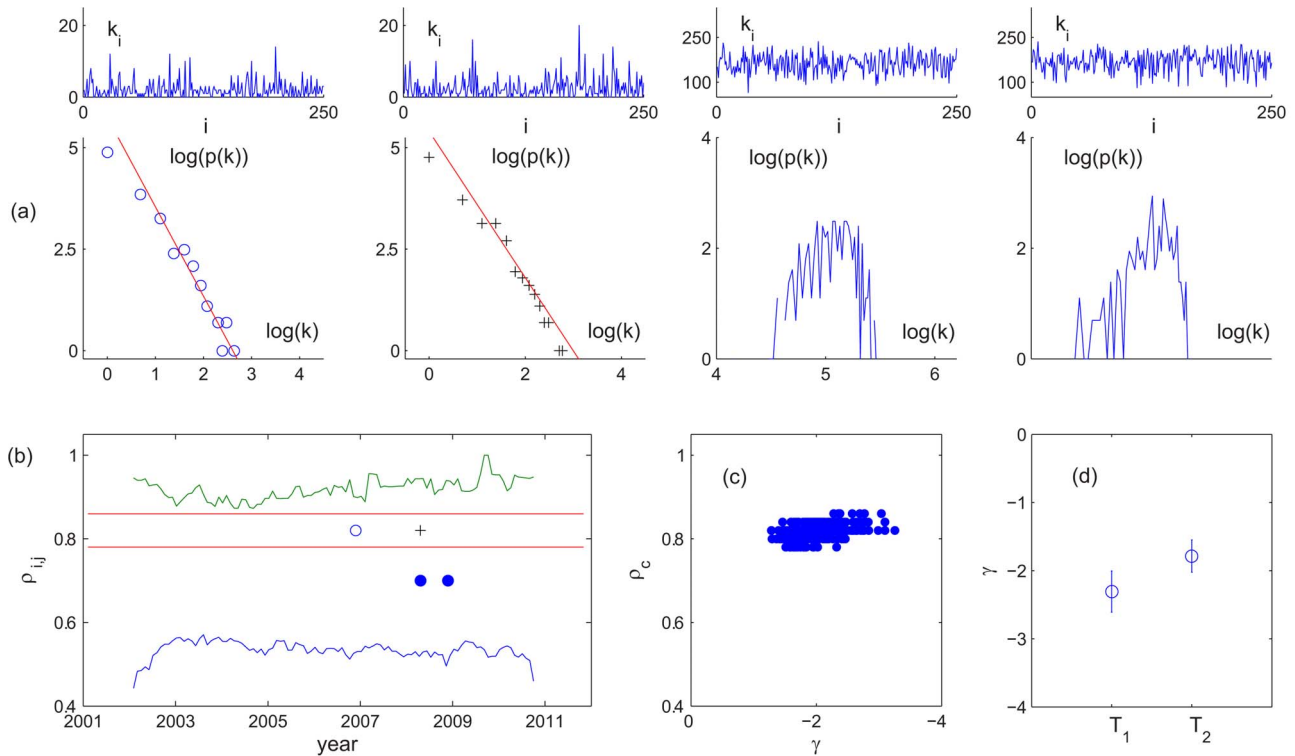


**Figure 5. Network characterization of FIS: degree of the network.** (a) Degree  $k_i$  and degree PDF of the price series, from left to right: 2007 Yr ( $\rho_c = 0.82$ , "o"), 2008 Yr ( $\rho_c = 0.82$ , "+"), and 2008 Yr, 2009 Yr ( $\rho_c = 0.7$ , "-"). The solid lines shown in the two left panels have the slope  $-2.2$  and  $-1.8$ , respectively. (b) The boundaries of the maximum (green) and minimum (blue) of  $\rho_{i,j}$  of the price series. The horizontal lines show the range of  $I_{SF}$  where  $p(k) \sim k^\gamma$ . The particular cases shown in (a) are also marked. (c) The exponent  $\gamma$  determined for  $\rho_c \in I_{SF}$  ( $\bullet$ ) where  $p(k) \sim k^\gamma$  is observed. (d) Average  $\gamma$  in the pre- and post-2008 regimes. The error bars correspond to one standard deviation.  
doi:10.1371/journal.pone.0077254.g005

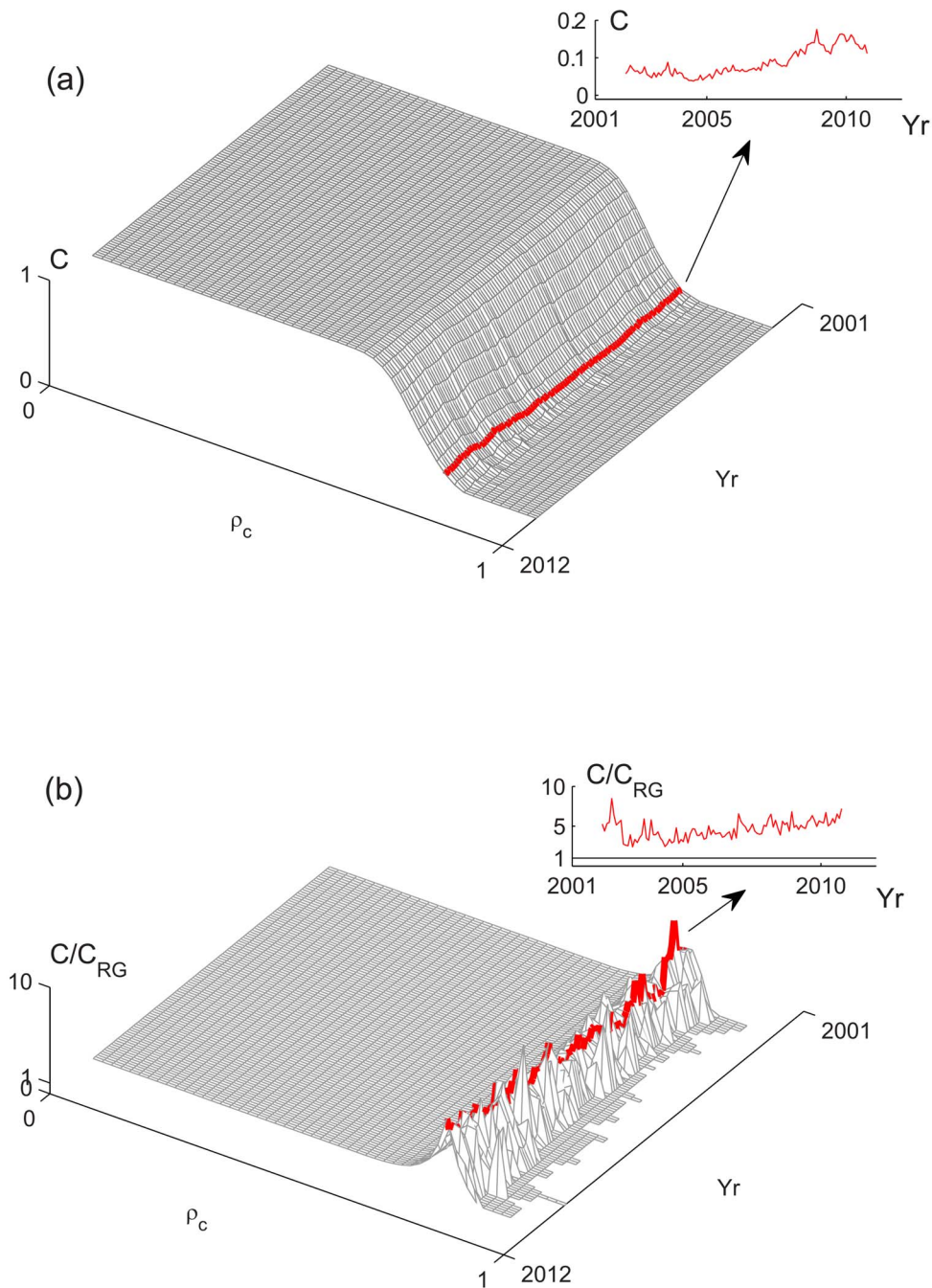


**Figure 6. Network characterization of FIS, clustering coefficient of the network.** (a) Clustering coefficient  $C$  and (b)  $C/C_{RG}$  as functions of  $\rho_c$  from 2001 to 2011. Typical results are shown for  $\rho_c = 0.82$ . The corresponding degree PDF's at 2007 ("o") and 2008 Yr ("+" have been shown in FIG. 5a.

doi:10.1371/journal.pone.0077254.g006

drop, showing the "return" of the market to its pre-2008 FIS level, while  $\sigma_\rho$  remains at a higher post-2008 level, showing the persistence of the market with a smaller cluster configuration.

These FIS characteristics, the market transition at  $T_*$  and the bifurcation pattern, are also captured by using different window parameters  $L=1, 1.5, 2, V=1$  (FIG. 3d), and using different number of price series (FIG. 3e). The robustness against these technical parameters supports a genuine market phenomenon in the analyzing period. For  $L=3$ , however, these characteristics are no longer found. Note, the "return" of the  $\mu_\rho$  value since the

second half of 2009 (FIG. 3c) suggests a  $\sim 2$  years "lifespan" for these FIS features. As a result, the missing of these characteristics using the  $L=3$  window segments should be due to averaging. In what follows, we will report results obtained by  $L=2, V=1$ .

It is reasonable to assume the action from traders has an immediate impact on the observed FIS in the price series. To examine this potential link, we also consider FIS from the daily returns. In particular, let  $r_i(t) = \log(x_{C,i}(t)/x_{O,i}(t))$  be the return during regular trading hours (9:30 am  $\sim$  4:00 pm) where  $x_{O,i}(t)$  is the opening price of the  $i$ th stock on the  $t$ th trading day. Consider

the cumulative daily return up till the trading day  $T$ ,  $S_{D,i}(T) = \sum_{t=1}^T r_i(t)$ , and the cumulative after-hour return (4:00 pm ~ 8:00 pm, 7:00 am ~ 9:30 am, E.T.),  $S_{AH,i}(T) = \sum_{t=2}^T \log(x_{O,i}(t)/x_{C,i}(t-1))$ . Note that subtle differences have been noted in the after-hour trading such as its lower liquidity, larger bid-ask spread [22]. Note, also, that

$$S_{AH,i}(T) = (-1)^{T-1} [S_{D,i}(T-1) - S_{D,i}(1) + \log(x_{C,i}(1)/x_{O,i}(T))]. \quad (1)$$

Hence, in terms of the fluctuation pattern, the after-hour  $S_{AH,i}$  may be viewed as a perturbation of the  $S_{D,i}$  by the opening price  $x_{O,i}(T)$ . As a result, these returns can exhibit qualitatively different FIS characteristics.

Similar to the price series, our result shows the same ascending trend in  $\mu_\rho, \sigma_\rho$  of the  $\{S_{D,i}\}$ ,  $\{S_{AH,i}\}$ , indicating a more synchronized trading action in the crisis development (FIG. 4). FIG. 4b shows the FIS indicators of  $\{S_{D,i}\}$  where similar FIS characteristics reported in FIG. 3 are observed. However, they are not found in the FIS indicators of  $\{S_{AH,i}\}$ . These results suggest a more direct impact to the market FIS from the regular-hour trading activities. That being the case, it is not possible to reject the significance of the after-hour trading in its entirety, since different trading characteristics in the pre-open (7:00 am ~ 9:30 am) and post-close (4:00 pm ~ 8:00 pm) are believed to exist [22]. However, we are not able to analyze these periods separately in the after-hour trading in this work.

In light of the above, we take a network approach to further characterize the FIS in the closing price. Here,  $x_{C,i}$ ,  $x_{C,j}$  are viewed as nodes and considered “connected” if  $\rho_{ij} > \rho_c$  for a threshold value  $\rho_c \in [0,1]$ . The degree of  $x_{C,i}$  in the network is then defined in the usual way by counting its links,  $k_i(\rho_c) = \#\{j, \rho_{ij} \geq \rho_c\}$  [23–26]. While no meaningful dynamics may be captured for  $\rho_c = 0$  ( $k_i \sim N$ ) or 1 ( $k_i \sim 0$ ), there exists an interesting  $\rho_c$  range,  $I_{SF}$ , where a scale free configuration is revealed with a power law degree PDF  $p(k) \sim k^{-\gamma}$  (dropping the subscript  $i$ ) (FIG. 5a). The exponent  $\gamma$  in the pre- and post-2008 regimes are averaged to  $\sim -2.2$  and  $\sim -1.8$ , respectively (FIG. 5d), indicating more links are formed in the post-2008 regime and, possibly, more clustering in the network. The latter can be confirmed from the clustering coefficient  $C_i(\rho_c)$ , which calculates the ratio of the number of links among  $x_{C,i}$ 's neighbors versus a fully connected neighborhood. We used the average  $C = \sum C_i/N$  to describe this property of the network as a whole. FIG. 6 shows  $C$  and  $C/C_{RG}$  as the function of  $\rho_c$  in the analyzing period, where  $C_{RG} = \langle k \rangle / N$  is the clustering coefficient of the random graph [23,26]. For  $\rho_c$  in  $I_{SF}$ ,  $C$  exhibits a similar rising trend as the FIS indicators through  $T_*$  (FIG. 6a). It follows intuitively that the rising FIS indicators imply more price series showing similar fluctuation pattern, which in turn leads to more clustering among the  $x_{C,i}$ 's. It is also seen a higher ratio  $C/C_{RG} > 3$  in the post-2008 regime, giving the evidence of a nontrivial networking structure underlying the market synchrony.

## Discussion and Conclusion

The notion of synchronized broadband processes in general should rest on the statistical ground of certain phase variable, and possibly be supported by the observation of similar fluctuation pattern. In this work, we adopt these premises to establish the preliminary ideas for synchrony in broad-band processes showing scale free characteristics. In particular, we propose using the

wavelet transform to associate the phase to the large amplitude jump characterized as the singularity. We then suggest the state of FIS with the assumption of a common mechanism underlying the singular fluctuation. While these ideas are successfully demonstrated using artificial examples, we stress the importance of the “selectiveness” of the analyzing wavelet in wavelet transform. When it is too sensitive, many WTMMs can emerge, which may be unrelated to the phase setting event leading to the large amplitude jump. We suggest using the wavelet that has the lowest number of vanishing moment, so as to associate the “most singular” fluctuation to the phase event.

The application of the proposed ideas to the market data leading to the 2008 financial crisis reveals several nontrivial results. The main implication of the findings is the significance of the market synchrony and its variability. The match of the rising FIS indicators  $\mu_\rho, \sigma_\rho$  to the approach of the 2008 financial crisis gives promise to using FIS to capture significant market events. In particular, our results imply many price series showing similar fluctuation pattern is a troubling sign. Considering  $\sigma_\rho$  as a function of  $\mu_\rho$  reveals a bifurcation pattern which suggests the transition towards a qualitatively different dynamical regimes in the crisis. It further implies that  $\sigma_\rho$ , the FIS variability, may be considered generally as an order parameter of the overall market dynamics.

Lillo and collaborators also suggest synchronous market activities based on the persistent bid-ask spread in the market limit orders [27–29]. The spread is significant since it creates a supply-demand unbalance which can lead to large price fluctuation. On that ground, the association of the singular fluctuation of the price to an underlying mechanism is well supported. In this work, we offer two modest extensions: (a) in addition to an individual stock, market synchrony is a global property that generally exists between different stocks, and (b) there is a likely link between a market in turmoil and excess FIS, and FIS variability.

Finally, we suggest that similar price fluctuation in a group of stocks without obvious business link reflects the herding or collective behavior of the traders [31–33]. To this end, we observe similar FIS characteristics in the regular trading hours, suggesting traders’ “collective motion” as a potential cause of the present findings. It is also in this realm that the market may be viewed as a “social” entity driven by a profit gaining objective. Indeed, market dynamics has been much discussed in such social context in the past; see [34,35] and references therein. Along these lines, we remark that our attempt of using a network analogy to characterize the dynamics underlying FIS has yielded similar  $\gamma$  and  $C$  values as other social networks reported in the past [23–26]. In general, we believe FIS describes a genuine property in complex dynamics and should be explored to uncover subtle interaction among the coupled oscillators in large dynamical systems.

## Supporting Information

**File S1.** The ticker symbols for the price series (DOCX)

## Acknowledgments

The author would like to thank anonymous referees for valuable comments.

## Author Contributions

Conceived and designed the experiments: DCL. Performed the experiments: DCL. Analyzed the data: DCL. Contributed reagents/materials/analysis tools: DCL. Wrote the paper: DCL.

## References

- Bennet M, Schatz MF, Rockwood H, Wiesenfeld H (2002) Huygens's clocks. *Proc. R. Soc. Lond. A* 458: 563–579.
- Boccaletti S, Kurths J, Osipov G, Valladares DL (2002) The synchronization of chaotic systems. *Phys. Rep.* 366: 1–101.
- Acebron JA, Bonilla LL, Perez Vicente CJ, Ritort F (2005) The Kuramoto model: a simple paradigm for synchronization. *Rev. Mod. Phys.* 77: 137–185.
- Krapivsky PL, Redner S (2003) Dynamics of majority rule in two-state interacting sping systems. *Phys. Rev. Lett.* 90: 238701.
- Galam S (2004) Contrarian deterministic effects on opinion dynamics: “the hung elections scenario.” *Physica A* 333: 453–460.
- de La Lama MS, Lopez JM, Wio HS (2005) Emergence of a contrarian-like effect in an opinion spreading model. *Europhys. Lett.* 72: 851–857.
- Hong H, Strogatz SH (2011) Kuramoto model of coupled oscillators with positive and negative coupling parameters: an example of conformist and contrarian oscillators. *Phys. Rev. Lett.* 106: 054102.
- Ranta E, Kaitala V, Lindstrom J, Linden H (1995) Synchrony in population dynamics. *Proc. R. Soc. Lond. B* 262: 113–118.
- Blasius B, Huppert A, Stone L (1999) Complex dynamics and phase synchronization in spatially extended ecological systems. *Nature* 399: 354–359.
- Cavagna A, Cimarelli A, Giardina I, Parisi G, Santagati R, et al. (2010) Scale-free correlations in starling flocks. *PNAS* 107: 11865–11870.
- Kerner BS (1998) Experimental features of self-organization in traffic flow. *Phys. Rev. Lett.* 81: 3797–3800.
- Lin DC, Sharif A, Kwan HC (2006) Scaling and organization of the EEG background activity and alpha rhythm in healthy young adults. *Biol. Cybern.* 95: 401–411.
- Ibarz B, Casado JM, Sanjuan MAF (2011) Map-based models in neuronal dynamics. *Phys. Rep.* 501: 1–74.
- Lin DC, Perez Velazquez JL, Nenadovic V (2012) Synchronous fluctuation in broad-band processes and application to the electroencephalographic brain data. *Europhysics Lett.* 97: 40001.
- Early accounts of such properties may be found in Mandelbrot BB (1967) The variation of some other speculative prices. *J. Bus.* 40: 393–413.
- Plerou V, Gopikrishnan P, Rosenow B, Amaral LAN, Stanley HE (2000) Econophysics: financial time series from a statistical physics point of view. *Physica A* 279, 433–456.
- Mallat S, Hwang WL (1992) Singularity detection and processing with wavelets. *IEEE Trans. Info. Theo.* 38: 617–643.
- Mallat S (1999) *A Wavelet tour of signal processing*. Academic Press.
- Muzy J, Bacry E, Arneodo A (1991) Wavelets and multifractal formalism for singular signals: application to turbulence data. *Phys. Rev. Lett.* 67: 3515–3518.
- Tass P, Rosenblum MG, Weule J, Kurths J, Pikovsky A, et al. (1998) Detection of n:m phase locking from noisy data: application to magnetoencephalography. *Phys. Rev. Lett.* 81: 3291–3294.
- Falconer (1990) *Fractal Geometry*, John Wiley & sons, New York.
- Barclay M, Hendershott T (2003) Price recovery and trading after hours. *Rev. Fin Studies* 16: 1041–1073.
- Albert R, Barabasi A-L (2002) Statistical mechanics of complex networks. *Rev. Mod. Phys.* 74: 47–97.
- Albert R, Jeong H, Barabasi A-L (1999) Diameter of the world wide web. *Nature* 401: 130–131.
- Wasserman S, Faust K (1994) *Social network analysis: methods and applications*. Cambridge Univ Press.
- Barabasi A-L, Albert R (1999) Emergence of scaling in random networks. *Science* 286: 509–512.
- Lillo F, Farmer JD, Mantegna RN (2003) Master curve for price-impact function. *Nature* 421:129–130.
- Lillo F, Farmer JD (2005) The key role of liquidity fluctuations in determining large price changes. *Fluct. Noise Lett.* 5: L209–L216.
- Moro E, Vicente J, Moyano LG, Gerig A, Farmer JD, et al. (2009) Market impact and trading profile of hidden orders in stock markets. *Phys. Rev. E* 80: 066102.
- Gode DK, Sunder S (1993) Allocative efficiency of markets with zero-intelligence traders: market as a partial substitute for individual rationality. *J. Political Econ.* 101: 119–137.
- Cont R, Bouchaud J-P (2000) Herd behavior and aggregate fluctuations in financial markets. *Macroecon. Dyn.* 4: 170–196.
- Eguiluz VM, Zimmermann MG (2000) Transmission of information and herd behavior: an application to financial markets. *Phys. Rev. Lett.* 85: 5659–5662.
- Corcos A, Eckmann J-P, Malaspina A, Malevergne Y, Sornette D (2002) Imitation and contrarian behaviour: hyperbolic bubbles, crashes and chaos. *Quant. Fin.* 2: 264–281.
- Coleman JS (1988) Social capital in the creation of human capital. *Am. J. Soc.* 94: S95–S120.
- Eguiluz VM, Zimmermann MG, Cela-Conde CJ, San Miguel M (2005) Cooperation and the emergence of role differentiation in the dynamics of social networks. *Am. J. Soc.* 110, 977–1008.